

# High Performance Silicon-on-Sapphire Subwavelength Grating Coupler for 2.7 $\mu$ m Wavelength

Jingjing Zhang, Junbo Yang, Wenjun Wu, Honghui Jia and Shengli Chang  
*Center of Material Science, National University of Defense Technology, Changsha 410073, China*

**Keywords:** Beam Splitter, Grating-Assisted Coupler, Coupled Mode Theory, Transfer Matrix Method.

**Abstract:** Couplers are important parts in integrated optical circuit and high efficiency compact couplers are in great demand. We report on high-efficiency silicon-on-sapphire (SOS) grating couplers at wavelength of 2.7 $\mu$ m. A 75% coupling efficiency and 50nm etching depth bandwidth (the tolerance of etching height) from a standard single-mode fiber to an SOS waveguide is obtained. A basic design principle of the grating coupler is presented, and some improved structures to enhance the coupling efficiency are proposed and estimated. The FDTD method is utilized to simulate and design the grating operated under TE polarization. With our optimization design, the coupling efficiency can be largely increased and beyond 80%. The gratings open the path to silicon photonic chips for the mid-infrared enabling new nonlinear optical functions as well as new spectroscopic lab on-a chip approaches.

## 1 INTRODUCTION

The mid-infrared (MIR) wavelengths, typically defined to range from 2-20 $\mu$ m (Saleh and Teich, 2007; Richard Soref, 2010; Richard A Soref et al., 2006), have proven to be useful for a number of applications. Many astronomy experiments depend upon the detection of MIR wavelengths (L. Labadie and O. Wallner, 2009). Chemical bond spectroscopy benefits from a large range of wavelengths from visible to past 20 $\mu$ m (H. B. Gray, 1994). Thermal imaging (such as night vision) depends upon mid-infrared wavelengths as a source of blackbody radiation (G. C. Holst and S. W. McHugh, 1992).

Silicon photonic waveguide circuits were originally conceived to be used for datacommunication and telecommunication applications (the wavelengths of 1.3 $\mu$ m and 1.55 $\mu$ m), a myriad of other application domains have emerged in recent years, including high performance mid-infrared optical systems operating in the 2-8 $\mu$ m spectral range<sup>7, 8</sup>. Working at these longer wavelengths reduces the parasitic nonlinear absorption in silicon, the two photon absorption, enormously. Without the two photon absorption we can fully benefit from the record nonlinear parameters obtained through the combination of the high linear index leading to high confinement and the high nonlinear index of silicon. The mid-IR is also a region in which second-and third-order

nonlinear optical effects can be exploited to great advantage. Thus, such systems could find applications in industrial and environmental monitoring (Willer et al., 2006), threat detection (Moore et al., 2004), medical diagnostics (Namjou et al., 2006) and free-space communication (Capasso et al., 2002).

The silicon-on-insulator (SOI) and silicon-on-sapphire (SOS) nanophotonic platform has been proposed as an excellent system for integrated mid-infrared (mid-IR) optical devices on account of the long wavelength transparency of silicon and many associated CMOS-compatible materials (Soref, 2008). Various methods have been explored for fabricating passive mid-IR waveguides and microcavities, with group-IV materials, including the use of "traditional" SOI rib and channel waveguides (G. Z. Mashanovich et al., 2001; M. M. Milošević et al., 2009), silicon-on-sapphire substrates (T. Baehr-Jones et al., 2010; A. Spott et al., 2010; F. Li et al., 2011).

Furthermore, numerous Si mid-IR components have been demonstrated, including ring resonators at 5.5 $\mu$ m (Mackenzie A. Van Camp et al., 2012), mid-infrared spectrometers (M. Muneeb et al., 2013), and grating coupler (B. Kuyken et al., 2011; Nannicha Hattasan et al., 2012; Zhenzhou Cheng et al., 2012; Ananth Z. Subramanian et al., 2012). In Ref 22, a grating couplers at wavelength of 2.15 $\mu$ m is demonstrated, which shows a peak

coupling loss of -5.2 dB. In following work (Nannicha Hattasan et al., 2012), a -3.8 dB coupling efficiency from a standard single-mode fiber to an SOI waveguide at  $2.1\mu\text{m}$  is obtained experimentally. In Ref 24, a TE mode shallow etched grating with coupling efficiency of 80.6% is predicted at the wavelength of  $2.75\mu\text{m}$  by finite-difference time-domain (FDTD) simulation. The coupling strength of mid-IR gratings can be tuned from 0.011 to 0.16 by changing the fill factor from 0.05 to 0.42. Authors use apodized structure in the front section of the grating, and uniform gratings for the rear section, thus, the design and fabrication is relatively difficult in practices. In addition, a grating coupler (using silicon nitride waveguide) at near-infrared wavelength is presented. An experimental efficiency of 5.7dB is reported (Ananth Z. Subramanian et al., 2012). Obviously, grating coupler at long wavelength is taken more and more attentions.

In this paper we propose a compact, simple and uniform structure grating coupler with 75% coupling efficiency at wavelength of  $2.7\mu\text{m}$ . The rigorous coupled wave theory is applied to the design and analysis of this coupler. Finally, the simulation results are obtained by the finite-difference time domain method.

## 2 PRINCIPLE AND DESIGN

Various grating couplers for coupling light between single mode fiber and submicron sized silicon waveguides have already been demonstrated at the  $1550\text{nm}$  telecom wavelength region (Junbo Yang et al., 2011; Junbo Yang et al., 2012; Dirk Taillaert, 2005). However the high absorption of silicon dioxide (for wavelength  $> 2.6\mu\text{m}$ ) greatly limits their applications in mid-infrared region. Therefore, we designed and fabricated the silicon coupler on SOS substrate. We optimize first the design parameters, including waveguide width, grating period, fill factor, grating widths, and grating height. A grating coupler can be obtained as shown in Fig. 1, which is composed of subwavelength pillars with uniform height.

The grating period is  $T$  and etching depth  $h$ . The thickness of waveguide and sapphire are  $H$  and  $W$ , respectively. A  $\theta=10^\circ$  tilt from vertical is presumed to avoid substantial second order Bragg reflection back into the waveguide when coupling to the optical fiber. The incident light  $P_{in}$  is divided into four parts throughout the grating:  $P_{co}$ ,  $P_{tr}$ ,  $P_{re}$  and  $P_{un}$ .  $P_{co}$  is the coupling power.  $P_{tr}$  is the transmission through the finite grating.  $P_{re}$  is the reflection at the grating.  $P_{un}$  is the power that is leaked down.  $P_{tr}$  can

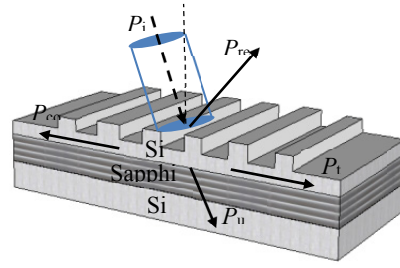


Figure 1: Schematic of fiber-to-chip grating coupler structure based on SOS.

be reduced to be very small after optimizing the structure and incident angle. So, we have:

$$P_{in} = P_{co} + P_{re} + P_{un} + P_{tr} \quad (1)$$

Coupling efficiency  $\eta$  is defined as:

$$\eta = \frac{P_{co}}{P_{in}} \quad (2)$$

The underlying sapphire thickness  $W$  has a major influence on the coupling efficiency. Its value is chosen in such a way that the downward radiated light which gets reflected at the sapphire/substrate interface interferes constructively with the direct upward radiated light. Based on this result the sapphire thickness  $W$  was fixed at  $0.88\mu\text{m}$  which can reduce leaked to the substrate to improve the grating couplers directionality.

For an SOS planar waveguide structure, we can obtain the effective refractive index (ERI) of the TE mode  $n_{eff}=2.318$ , we use Rsoft to compute  $n_{eff}=2.318$  when the thickness of the waveguide  $H$  is  $220\text{nm}$  (The limited thickness of TE<sub>0</sub> mode)  $\lambda = 2.7\mu\text{m}$  as shown in Fig.2.

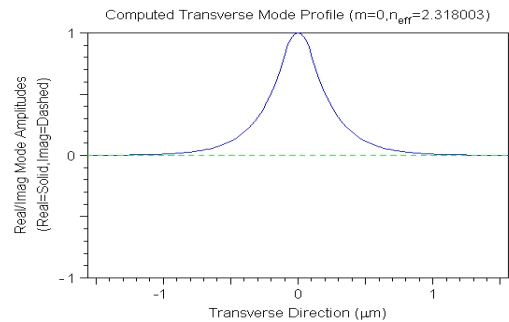


Figure 2: The profile of waveguide mode.

Next, according to the phase match condition between the gratings and the waveguide mode:

$$T \times (n_{eff} - n_{clad} \cdot \sin\theta) = m\lambda \quad (3)$$

$$m = 0, \pm 1, \pm 2 \dots$$

Where  $n_{clad}=1$  (air) and the grating period  $T$  is equal

to 1.2603 $\mu\text{m}$ . In addition, the fill factor of grating  $f$  which defined as the ratio of pillar width to grating period is equal to 0.4. We can control the width of each pillar to obtain the desired refractive index distribution. With the calculations given above, finally, all the parameters required for constructing a subwavelength grating coupler based on SOS is listed in Table.1.

Table.1: Design parameters of grating coupler (Unit: Micrometers).

Parameters	$\lambda$	$T$	$h$	$H$	$W$	$f$	$\theta$
Value	2.7	1.2603	0.12	0.22	0.88	0.4	10 $^\circ$

Simultaneously, the finite-difference time-domain method, a powerful and accurate method for a finite-size structure, is chosen to simulate and design this device. For a 2.7 $\mu\text{m}$  wavelength, the coupling efficiency is about 75% when we consider the TE. The  $E_y$  component of optical field is given in Fig. 3.

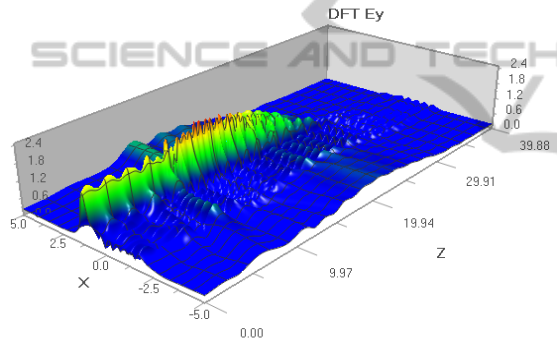


Figure 3: Distribution of optical field.

According to above theoretical analysis, we take these parameters given in Table 1 as a starting point to simulate and evaluate the performance of the grating coupler described above. We will look at the sensitivity of the grating couplers to variations in the grating parameters. We introduce errors on the etch depth, filling factor and grating width (period tolerance).

In fabrication, considering requirements of production process, the grating depth is hard to control because electron beam density which is hard to control current on the accuracy of the etching depth. We will evaluate the influence of fabrication error to the coupling efficiency. The resulting coupling efficiency as a function of etching depth is shown in Fig. 4.

It shows a maximum coupling efficiency around 75% (grating depth  $h=0.12\mu\text{m}$ ) and a 1 dB depth bandwidth of 50 nm (from 0.1 $\mu\text{m}$  to 0.15 $\mu\text{m}$ ). When the grating height is larger than 0.26 $\mu\text{m}$  or lower than 0.06 $\mu\text{m}$ , the mismatch of mode profile between

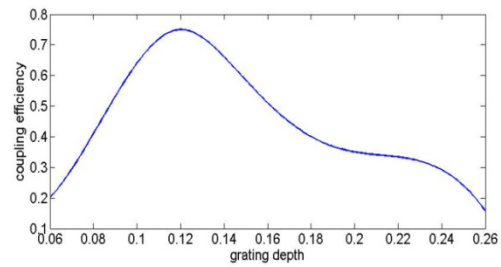


Figure 4: Coupling efficiency as a function of grating depth with  $\lambda=2.7\mu\text{m}$ ,  $T=1.2603\mu\text{m}$ ,  $f=0.4$ ,  $\theta=10^\circ$ .

grating field and fiber will be large. Consequently, if the grating is etched too deep or too shallow the wavelength is obviously shifted to longer or shorter wavelengths (not shown in Fig.4), and the second order reflection is also increased. So the coupling efficiencies are significantly low.

Fig.5 shows the effect of a different filling factor. It shows a maximum coupling efficiency around 75% with grating depth  $f=0.4\mu\text{m}$ . Changing it from 0.4 to 0.35 or 0.45 has only a small effect on the coupling efficiency curves, in which the coupling efficiency is larger than 60%.

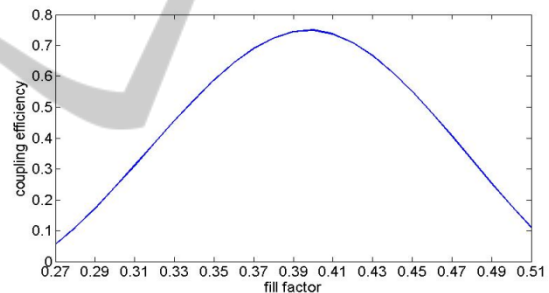


Figure 5: Coupling efficiency as a function of fill factor with  $\lambda=2.7\mu\text{m}$ ,  $T=1.2603\mu\text{m}$ ,  $h=0.12\mu\text{m}$ ,  $\theta=10^\circ$ .

Fig.6 shows the coupling efficiency as a function of angle. The  $\theta=10^\circ$  curve has a maximum for  $\lambda=2.7\mu\text{m}$ . The case of vertical coupling ( $\theta=0^\circ$ ) is very interesting from a practical point of view. However, as above mentioned, in such case, the second order diffraction is reflecting back into the waveguide, which results in the coupling efficiency obviously degenerated.

The effect of random errors on the groove widths is shown in Fig.7. The coupling efficiency gets its maximum value when the grating period error is 0 ( $T=1.2603\mu\text{m}$ ). The errors have a normal (Gaussian) distribution with half width 40nm (from -20nm to 20nm). Compared to the perfect structure, the coupling efficiency is obviously reduced to the half of the maximum.

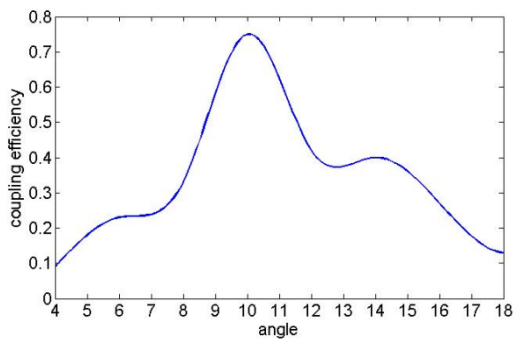


Figure 6: Coupling efficiency as a function of incidence angle with  $\lambda=2.7\mu\text{m}$ ,  $T=1.2603\mu\text{m}$ ,  $h=0.12\mu\text{m}$ ,  $f=0.4$ .

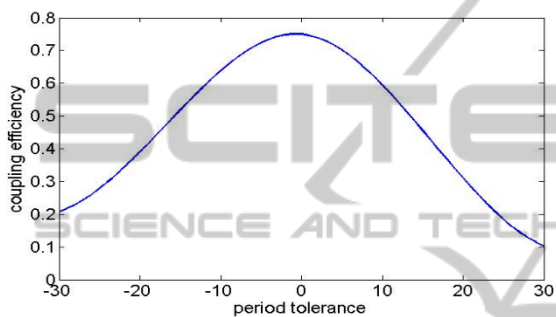


Figure 7: Influence of period tolerance on coupling efficiency with  $\lambda=2.7\mu\text{m}$ ,  $h=0.12\mu\text{m}$ ,  $f=0.4$ ,  $\theta=10^\circ$ .

In real fabricated structures these errors on the different parameters are present all at the same time. In the worst case scenario everything adds up, but it is also possible that one error cancels the other. We can conclude that the tolerances to fabrication errors are very tight, but achievable. The high accuracy needed is typical for all nanophotonic structures.

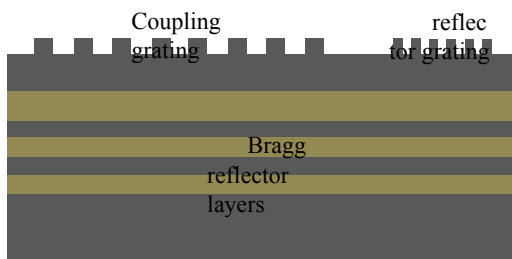


Figure 8: Optimized grating coupler using reflector grating and Bragg reflection layers.

As above discussed, at the coupler grating, part of the light is reflected  $P_{re}$ , part is coupled out  $P_{co}$ , part is transmitted  $P_{tr}$  and the rest is leaked down to substrate  $P_{un}$ . In order to improve the coupling efficiency, one way is to add a second grating with the same etch depth as the coupler grating, which

acts as a reflector behind the coupler grating as shown in Fig.8. If the structure is properly designed which the direct reflection at the coupler grating and the reflection from the reflector grating interfere destructively, it is possible to reduce the reflection at the coupler and couple all light out. Simultaneously, a bottom reflector can further improve the coupling efficiency to fiber. This bottom reflector can be a multi-layer dielectric mirror or a metal mirror. We have chosen for a Bragg reflection layers consisting of Si/Sapphire pairs. The thickness of each layer  $t=\lambda/4n$  must be well controlled to obtain a high reflectivity.  $n$  is the refractive index of the layer of silicon and sapphire. Thanks to the high refractive index contrast, only a few pairs are needed and the reflection is broadband. Depend on above optimized methods, the coupling efficiency beyond 80% can be realized for mid-infrared wavelength.

#### 4 CONCLUSIONS

In this paper, we proposed a subwavelength grating coupler with coupling efficiencies exceeding 75% at a wavelength of  $2.7\mu\text{m}$  with an 50nm depth bandwidth of 1dB. The coupling efficiency can reach up to about 80% if the optimized method is adopted. The gratings open the path to silicon photonic chips for the mid-infrared enabling new nonlinear optical functions as well as new spectroscopic lab on-a chip approaches. Experiments are being carried out and results will be presented soon.

#### ACKNOWLEDGEMENTS

This work was supported by the National Natural Science Foundation of China (60907003), the Foundation of NUDT (JC13-02-13), the Hunan Provincial Natural Science Foundation of China (13JJ3001), and Program for New Century Excellent Talents in University (NCET-12-0142). The authors gratefully acknowledge helpful discussions with Prof. Zhiping Zhou.

#### REFERENCES

B. E. A. Saleh and M. C. Teich, *Fundamentals of Photonics* (John Wiley & Sons, Inc., 2007), p.39.  
 Richard Soref, Mid-infrared photonics in silicon and germanium, *Nature Photonics*, 4, 495-497, 2010.  
 Richard A Soref, Stephen J Emelett and Walter R Buchuald, Silicon waveguided components for the

- long-wave infrared region, *Journal of Optics A: Pure and Applied Optics*, 8, 840-848, 2006.
- L. Labadie, and O. Wallner, Mid-infrared guided optics: a perspective for astronomical instruments, *Opt. Express* 17, 1947-1962, 2009.
- H. B. Gray, *Chemical Bonds: An Introduction to Atomic and Molecular Structure* (University Science Books), 1994.
- G. C. Holst and S. W. McHugh, Review of thermal imaging system performance, *Proceedings of SPIE*, 78-84, 1992.
- Xiaoping Liu, Bark Kuyken, Gunther Roelkens, Roel Baets, Richard M. Osgood Jr, William M.J.Green, Bridging the mid-infrared-to-telecom gap with silicon nanophotonic spectral translation, *Nature Photonics*, 23, 667-671, 2012.
- Jalali, B. et al. Prospects for silicon mid-IR Raman lasers. *IEEE J. Sel. Top. Quantum Electron.* 12, 1618-1627 (2006).
- Willer, U., Saraji, M., Khorsandi, A., Geiser, P. & Schade, W. Near- and mid-infrared laser monitoring of industrial processes, environment and security applications. *Opt. Laser Eng.* 44, 699-710 (2006).
- Moore, D. S. Instrumentation for trace detection of high explosives. *Rev. Sci. Instrum.* 75, 2499-2512 (2004).
- Namjou, K., Roller, C. B. & McCann, P. J. The Breathmeter: a new laser device to analyze your health. *IEEE Circ. Dev. Magazine* 22-28 (2006).
- Capasso, F. et al. Quantum cascade lasers: ultrahigh-speed operation, optical wireless communication, narrow linewidth, and far-infrared emission. *IEEE J. Quantum Electron.* 38, 511-532 (2002).
- R. Soref, Towards silicon-based longwave integrated optoelectronics (LIO), *SPIE Proc.* 6898, 689809, 689809-13 (2008).
- G. Z. Mashanovich, M. M. Milošević, M. Nedeljkovic, N. Owens, B. Xiong, E. J. Teo, and Y. Hu, Low loss silicon waveguides for the mid-infrared, *Opt. Express* 19(8), 7112-7119 (2011).
- M. M. Milošević, P. S. Matavulj, P. Y. Yang, A. Bagolini, and G. Z. Mashanovich, Rib waveguides for midinfrared silicon photonics, *J. Opt. Soc. Am. B* 26(9), 1760-1766 (2009).
- T. Baehr-Jones, A. Spott, R. Ilic, A. Spott, B. Penkov, W. Asher, and M. Hochberg, Silicon-on-sapphire integrated waveguides for the mid-infrared, *Opt. Express* 18(12), 12127-12135 (2010).
- A. Spott, Y. Liu, T. Baehr-Jones, R. Ilic, and M. Hochberg, Silicon waveguides and ring resonators at 5.5  $\mu$ m, *Appl. Phys. Lett.* 97(21), 213501 (2010).
- F. Li, S. D. Jackson, C. Grillet, E. Magi, D. Hudson, S. J. Madden, Y. Moghe, C. O'Brien, A. Read, S. G. Duvall, P. Atanackovic, B. J. Eggleton, and D. J. Moss, Low propagation loss silicon-on-sapphire waveguides for the mid-infrared, *Opt. Express* 19(16), 15212-15220 (2011).
- Yang Liu, Alexander Spott, Tom Baehr-Jones, Rob Ilic, Michael Hochberg, Silicon waveguides and ring resonators at 5.5 $\mu$ m, *Group IV Photonics(GFP)*, 2010 7<sup>th</sup> IEEE International Conference.
- Mackenzie A. Van Camp, Solomon Assefa, Douglas M. Gill, Tymon Barwicz, Steven M. Shank, Philip M. Rice, Teya Topuria, and William M. J. Green1, Demonstration of electrooptic modulation at 2165nm using a silicon Mach-Zehnder interferometer, *Optics Express*, 20(27), 28009-28016, 2012.
- M. Muneeb, X. Chen, P. Verheyen, G. Lepage, S. Pathak, E. Ryckeboer, A. Malik, B. Kuyken, M. Nedeljkovic, J. Van Campenhout, G. Z. Mashanovich, and G. Roelkens, Demonstration of Silicon-on-insulator midinfrared spectrometers operating at 3.8 $\mu$ m, *Optics Express*, 21(10), 11659-11669, 2013.
- B. Kuyken, N. Hattasan, D. Vermeulen, S. Selvaraja, W. Bogaerts, W. M. J. Green, R. Baets, G. Roelkens, Highly Efficient Broadband Silicon-on-Insulator Grating Couplers for the Short Wave Infrared Wavelength Range, *OSA/ANIC/IPR/Sensors/SL/SOF/SPPCom/2011*
- Nannicha Hattasan, Bart Kuyken, Francois Leo, Eva M. P. Ryckeboer, Diedrik Vermeulen, and Gunther Roelkens, High-Efficiency SOI Fiber-to-Chip Grating Couplers and Low-Loss Waveguides for the Short-Wave Infrared, *IEEE Photonics Technology Letters*, 24(17), 1536-1538, 2012.
- Zhenzhou Cheng, Xia Chen, C. Y. Wong, Ke Xu, Christy K. Y. Fung, Y. M. Chen, Hon Ki Tsang, Mid-Infrared Grating Couplers for Silicon-on-Sapphire Waveguides, *IEEE Photonics Journal*, 4(1), 104-113, 2012.
- Ananth Z. Subramanian, Shankar Selvaraja, Peter Verheyen, Ashim Dhakal, Katarzyna Komorowska, and Roel Baets, Near-Infrared Grating Couplers for Silicon Nitride Photonic Wires, *IEEE Photonics Technology Letters*, 24(19), 1700-1703, 2012.
- Junbo Yang, Zhiping Zhou, XinJun Wang, Danhua Wu, Huaxiang Yi, JianKun Yang, and Wei Zhou, Compact double-layer subwavelength binary blazed grating 1 $\times$ 4 splitter based on silicon-on-insulator, *Optics Letters*, 36(6), 837-839, 2011.
- Junbo Yang, Zhiping Zhou, Honghui Jia, Xueao Zhang, and ShiQiao Qin, High-performance and compact binary blazed grating coupler based on an asymmetric subgrating structure and vertical coupling, *Optics Letters*, 36(14), 2614-2616, 2012.
- Dirk Taillaert, *Grating couplers as Interface between Optical Fibres and Nanophotonic Waveguides*, Gent University, 2005.